

Comparative Time-Series Analysis of Hip and Shoulder Rotation in Baseball Bat Swings

Koga Okubo, Kanta Tachibana, *

March 11, 2025

Abstract

This study focuses on the rotation of the hips and shoulders during a baseball bat swing, analyzing the time-series changes in rotational angles, rotational velocities, and axes using marker position data obtained from a motion capture system with 12 infrared cameras. Previous studies have examined factors such as ground reaction forces, muscle activation patterns, rotational energy, angular velocity, and angles during a swing. However, to the best of our knowledge, the hip and shoulder rotational motions have not been adequately visualized or compared. In particular, there is a lack of analysis regarding the coordination and timing differences between hip and shoulder movements during the swing. Therefore, this study aims to quantitatively compare the hip and shoulder rotational movements during the swing between skilled and unskilled players and visualizes the differences between them. Based on the obtained data, the study aims to improve the understanding of bat swing mechanics by visualizing the coordinated body movements during the swing.

1 Introduction

Baseball batting motions vary widely among hitters and can change even for the same hitter depending on his physical condition. Previous studies [1–4] have investigated baseball bat swings. Hirayama et al. [1] analyzed bat swing velocity and trunk rotation angles using 3D motion data, ground reaction force (GRF) using a force plate, and lower limb muscle load patterns using a musculo-skeletal model. They compared nine skilled players selected from a technical college baseball team with seven unskilled first-year substitute players. Isogai et al. [2] measured the GRF of the pivot and stance foot using a force plate. They divided the swing motion into four phases—stance, take-back, impact, and follow-through—and compared six male baseball players from the same technical college with six male students who were not part of the baseball team. Horiuchi

*K. Okubo and K. Tachibana were with the Department of System Mathematics Science, School of Informatics, Kogakuin University, Japan e-mail:jx21055@g.kogakuin.jp, kanta@cc.kogakuin.ac.jp.

et al. [3] measured swing speed with 11 university baseball players as subjects. Reflective markers were placed on the toes and heels of both feet, the tip of the bat, and the grip of the bat, and data were collected using a 3D motion analysis system. Fang et al. [4] extracted the center of mass trajectory of the body during the swing from 2D images and compared subjects. However, the studies [1,3] did not visualize or compare the kinematic time-series patterns of hip and shoulder rotation. In addition, the study [2] only evaluated the maximum, minimum, and impact values of GRF in the four swing phases, without analyzing rotational movements related to body coordination. Furthermore, study [4] estimated data from 2D images rather than using 3D motion data.

There have also been studies of body coordination during baseball-like swing motions, such as swinging a racket, bat or club. The kinetic chain is critical in swing motions. Studies [5–8] have analyzed upper body coordination during tennis racket swing. Ishikawa and Murakami [5] studied mechanical energy and energy transfer patterns in different body segments during racket swing using inertial measurement units (IMUs) attached to seven upper body locations of three tennis players. Zhao et al. [6] used motion sensors attached to the racket handle to estimate the ball speed for three types of shots—serves, ground strokes, and volleys. Özçelik [7] compared the hit rate at the racket’s sweet spot of the racket between forehand and backhand strokes. However, the studies [6,7] examined only swing speed and accuracy without investigating the kinetic chain responsible for the racket movement. Ebner et al. [8] analyzed 3D acceleration and angular velocity data from IMU sensors placed at the wrist, forearm, upper arm, and shoulder for eight types of tennis strokes.

Golf swing motion has also been studied. Studies [9–12] measured acceleration and angular velocity at two locations on the upper and lower back during golf swings. Reintrakulchai and Kimpan [9] used these data to compare a coach with four students. Kim, Zohdy, and Barker [10] analyzed amateur golfers’ swings using pose estimation techniques to assess body coordination based on posture at key frames, swing tempo, and consistency. Zhang et al. [11] applied machine learning to golf swing data from four skilled golfers, analyzing individual identification based on five body parts. Kim et al. [12] evaluated body coordination by analyzing golf swing movements from five body parts using wrist-worn IMU bands.

The kinetic chain during cricket swings has also been studied. Curtis et al. [13] used a motion capture system to record the head, both feet, and bat positions, and then applied fuzzy logic to compare body coordination between skilled and unskilled batsmen from six perspectives, including shoulder and hip movement. Bandara and Bačić [14] classified batting strokes based on five coordinate points extracted from cricket batting videos. Gajanayake et al. [15] developed a custom IMU device to measure and record bat movement in real time during swings. Mohonta and Sarkar [16] used bat-mounted inertial sensors attached to a bat to measure ten consecutive swings and analyzed the batting motion using a pendulum model to evaluate swing characteristics and performance.

Among studies of body coordination during bat, rackets, or club swings

similar to baseball batting, studies [8, 11, 14, 15] focused on shoulder rotation. Studies [9, 10, 12] examined coordination between hip and shoulder movements. However, none of these studies simultaneously visualized and compared the temporal patterns of hip and shoulder rotation. Therefore, the lack of a comprehensive time-series visualization and comparison of hip-shoulder coordination in skilled and unskilled players remains an important gap in the literature.

2 Theoretical Background

Human body movements are driven by external forces, including GRF, gravity, and skeletal muscle contractile forces of skeletal muscles, which generate acceleration and angular acceleration in body segments. These forces are then converted into rotational kinetic energy by bones and joints. In a baseball bat swing, body segments move sequentially, transferring energy from the lower limbs to the pelvis, trunk, and upper limbs using GRF. This kinetic chain is essential to produce an efficient swing motion. Taguchi et al. [17] pointed out that differences in bat swings affect the load on the spine and that the timing of rotational angular velocity and acceleration is critical to maximizing bat power.

Based on these findings, bat swings are movements that are strongly influenced by both mechanical principles and physiological characteristics. The analysis of hip and shoulder rotational movements during a bat swing is important for improving athletic performance and preventing injuries. Therefore, this study focuses on hip and shoulder rotation.

3 Method and Experiments

This study uses a motion capture system with a set of markers placed at a total of 16 locations on the body: the temples, the head, both wrists, both elbows, both shoulders, both hips, both knees, both ankles, and both toes. Fig. 1 illustrates the marker locations used for measurement.

The motion capture system had a frame rate of 60 fps. Fig. 2 shows the coordinate system of the motion capture system. As shown in Fig. 2, the coordinate system is defined as follows: the $+y$ axis points vertically upward, the $+z$ axis extends from home plate toward the pitcher’s mound, and the $+x$ axis follows the right-hand rule, perpendicular to both.

In this study, the swings of four subjects were measured: two registered players from the Tokyo New University Baseball League Division II (one left-handed and one right-handed) and two unregistered individuals (one left-handed and one right-handed). Hereafter, they are referred to as "skilled" and "unskilled" batters. All four subjects used a 170g plastic bat during the swings. During the swing, the rotational angular velocities $\omega_h(\geq 0)$ and $\omega_s(\geq 0)$ [deg/s] of hip and shoulder, respectively, are calculated for each frame. And the 3D rotational axis vectors of the hip \vec{a}_h and the shoulder \vec{a}_s are calculated, where $|\vec{a}_h| = |\vec{a}_s| = 1$.

For frame n , the vector $\vec{h}(n)$ is defined as from the right hip marker to the

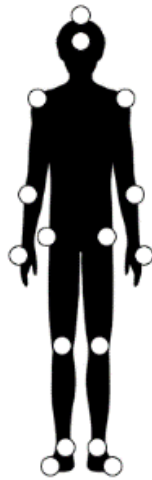


Figure 1: Positions of reflective markers.

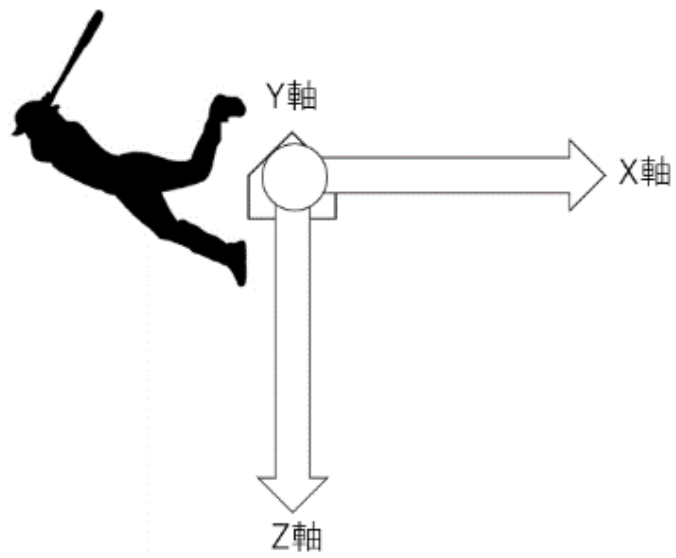


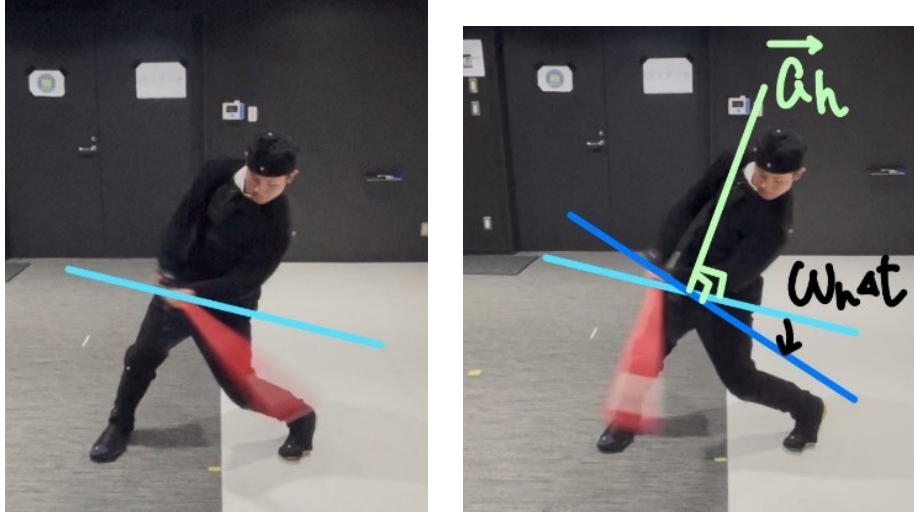
Figure 2: Coordinate system.

left hip marker. The ω_h and \vec{a}_h are calculated to satisfy eq. (1). Similarly, defining the vector $\vec{s}(n)$ from the right shoulder marker and the left shoulder marker, the ω_s and \vec{a}_s are calculated so that they satisfy eq. (2).

$$\sin(\omega_h(n)\Delta t)\vec{a}_h(n) = \frac{\vec{h}(n) \times \vec{h}(n+1)}{|\vec{h}(n)||\vec{h}(n+1)|}, \quad (1)$$

$$\sin(\omega_s(n)\Delta t)\vec{a}_s(n) = \frac{\vec{s}(n) \times \vec{s}(n+1)}{|\vec{s}(n)||\vec{s}(n+1)|}, \quad (2)$$

where, \times shows the cross product of 3D vectors and the frame interval $\Delta t = \frac{1}{60}$ [s].



(a) Hip vector $\vec{h}(17)$

(b) $\vec{h}(18)$, $\vec{a}_h(17)$ and $\omega_h(17)$

Figure 3: Hip rotation speed and axis from frame 17 to frame 18.

The inclination angle $\varphi_h(n)$ of the hip's plane of rotation relative to the horizontal plane is calculated for frame n .

$$\cos(\varphi_h(n)) = \vec{e}_y \cdot \vec{a}_h(n),$$

$$\cos(\varphi_s(n)) = \vec{e}_y \cdot \vec{a}_s(n),$$

where \vec{e}_y is the unit vector pointing vertically downward for left hitter and upward for right hitter. The time-series graphs of $\varphi_h(n)$ and $\varphi_s(n)$ are compared between skilled and unskilled players. The similarities and differences are analyzed and discussed.

4 Results

The results of the experiments on the rotation angle, rotation angular velocity, and axis of rotation axis are described. This experiment was conducted with four participants, two each with and two without baseball experience.

4.1 Horizontal Rotation Angle

Fig. 4 defines the shoulder rotation angle $\theta_s(n)$ [deg] in the horizontal plane. Similarly, the hip rotation angle $\theta_h(n)$ is defined with the $+z$ -direction as 0 [deg] and is measured clockwise when viewed from above. In Fig. 4, the angle between the vector $\vec{s}(n)$ projected onto the horizontal plane and the $+z$ -direction is shown blue.

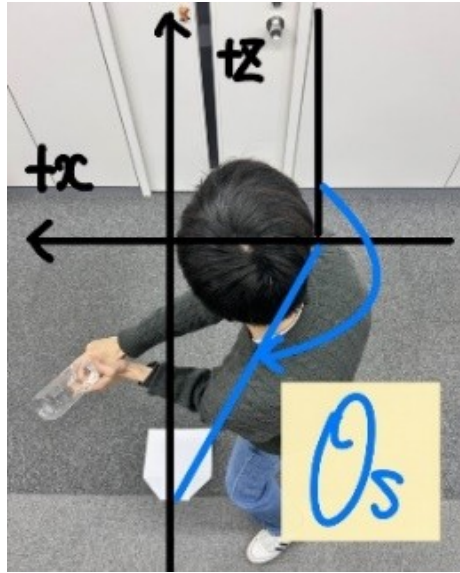


Figure 4: Definition of shoulder rotation angle θ_s in the horizontal plane.

The beginning frame of batting motion is defined as that at which either of the hip or shoulder rotation starts, i.e., the Y-component of the rotation axis vector becomes positive for right-handed batters and negative for left-handed batters. Also, the end frame of batting motion is defined that the last frame of the rotation continues for either hip or shoulder. Figs. 5 and 6 show the hip and shoulder rotation angles in the horizontal plane for skilled players. The horizontal axis represents the frame. The vertical axis represents the angle in the horizontal plane. Figs. 7 and 8 show the hip and shoulder rotation angles for unskilled players.

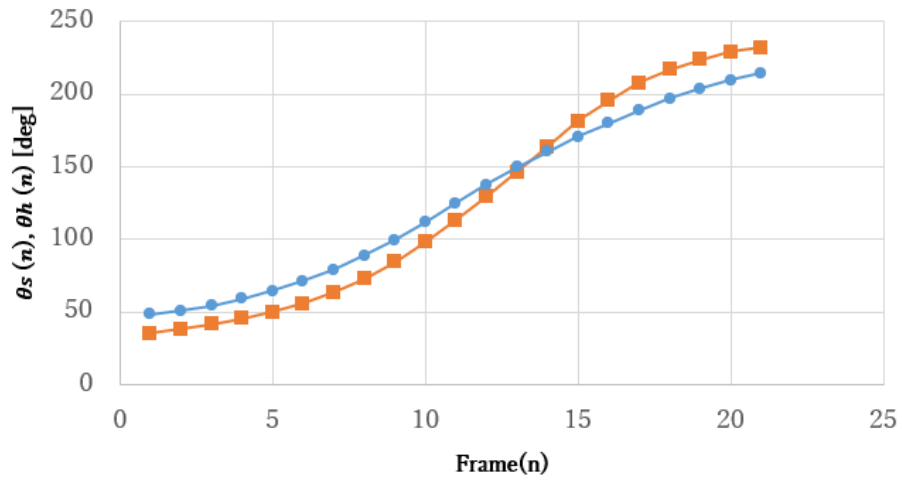


Figure 5: Horizontal rotation angle of hip (blue) and shoulder (orange) in the skilled left batter.

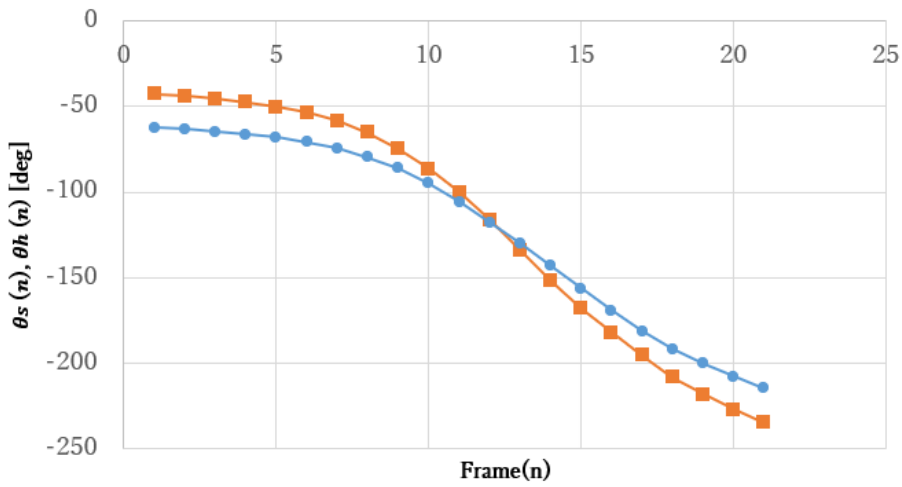


Figure 6: Horizontal rotation angle of hip (blue) and shoulder (orange) in the skilled right batter.

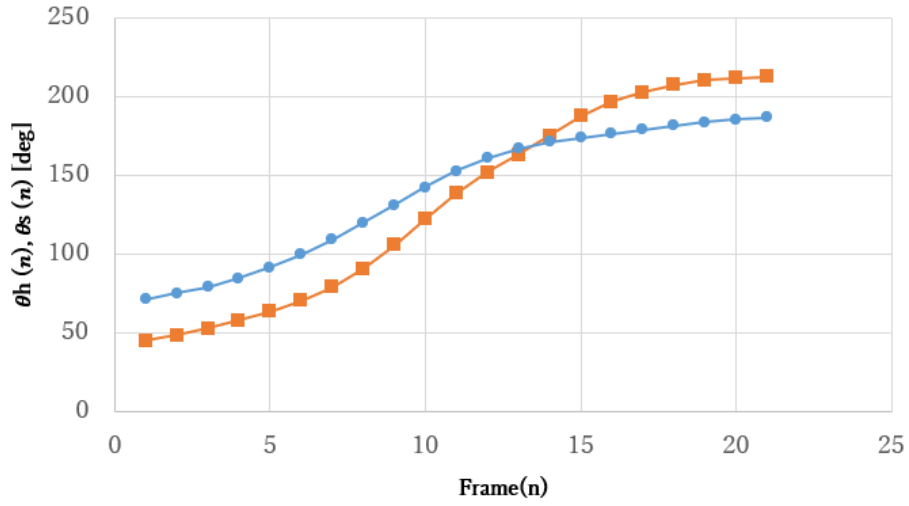


Figure 7: Horizontal rotation angle of hip (blue) and shoulder (orange) in the unskilled left batter.

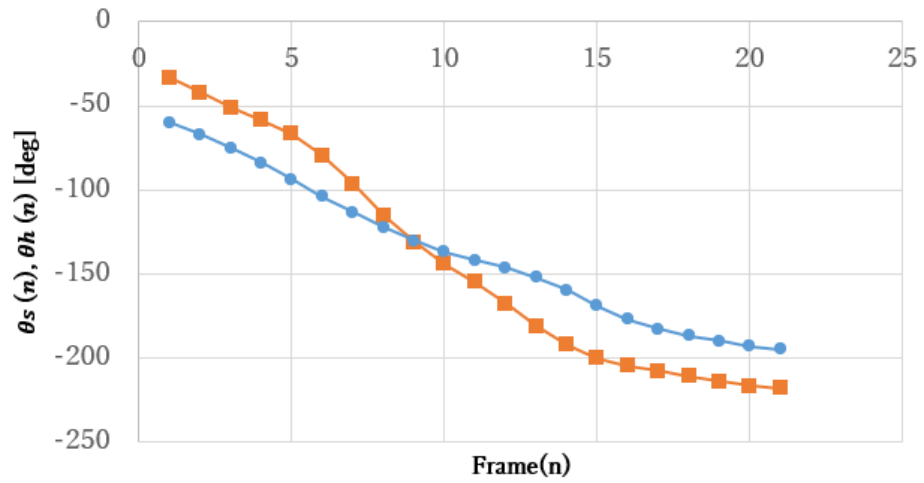


Figure 8: Horizontal rotation angle of hip (blue) and shoulder (orange) in the unskilled right batter.

4.2 Rotation Speed

Figs. 9 and 10 show the hip and shoulder rotation speed during the swing for skilled players. In these figures, the horizontal axis represents the frame number. The vertical axis represents the rotation speed [deg/s]. The blue line represents the hip rotation speed, and the orange line represents the shoulder rotation speed. The black vertical line marks the frame just before the wrist snap during the swing. Similarly, Figs. 11 and 12 show the rotation speed for unskilled players.

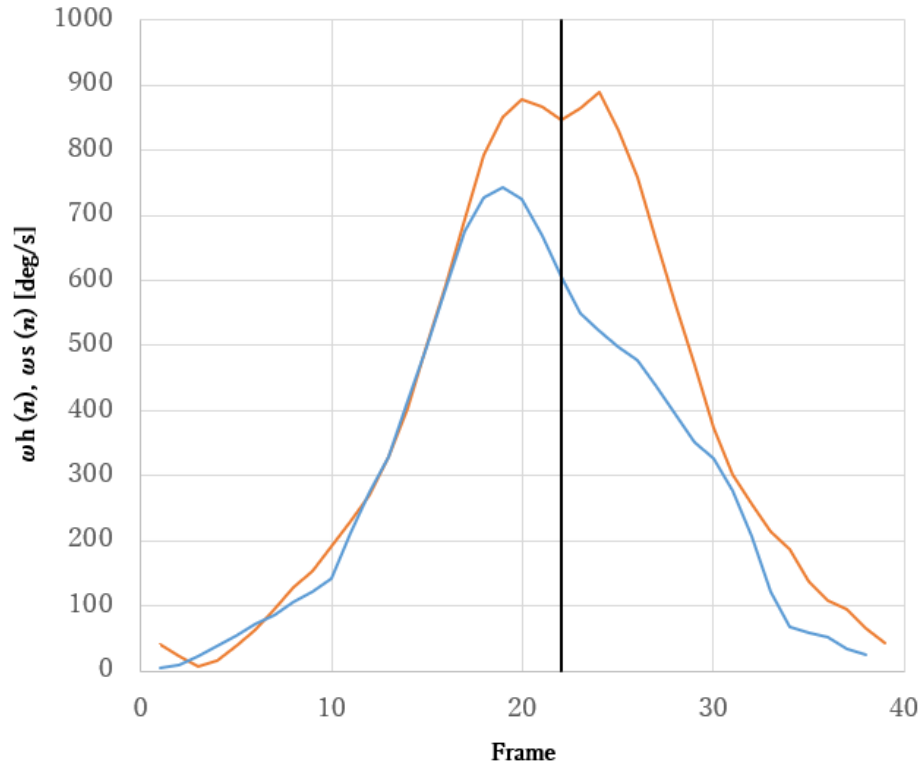


Figure 9: Rotation speed of hip (blue) and shoulder (orange) in the skilled left batter.

4.3 Rotation Axis

Figs. 13 and 14 show the angle [deg] between the rotation plane and the horizontal plane for the skilled players. The 10 frames before and 10 frame after the wrist snap frame, a total of 21 frames are shown. In these figures, the blue line represents the inclination of hip rotation plane θ_h . The orange line represents that of shoulder rotation plane θ_s . The black vertical line marks the frame just

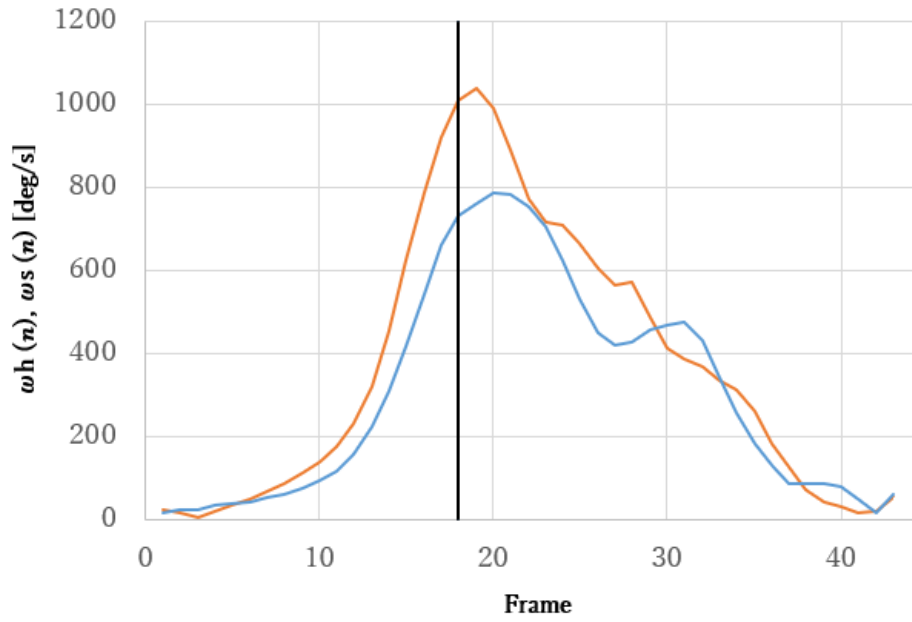


Figure 10: Rotation speed of hip (blue) and shoulder (orange) in the skilled right batter.

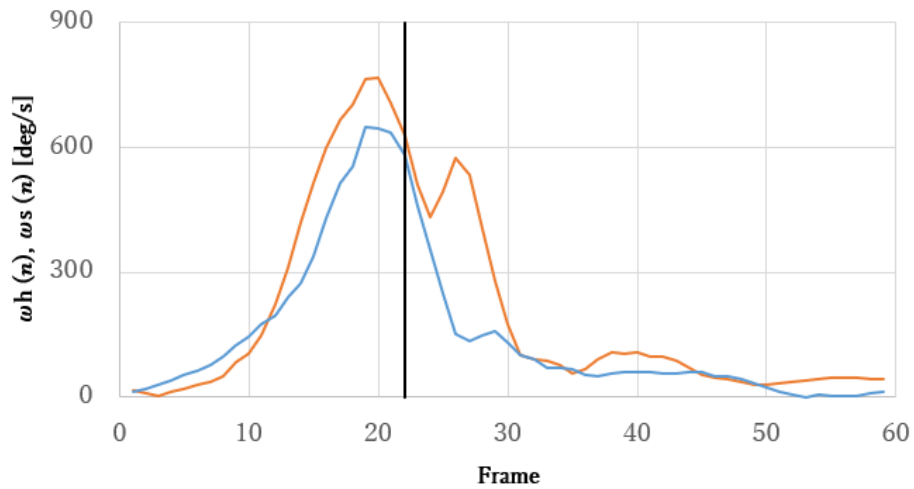


Figure 11: Rotation speed of hip (blue) and shoulder (orange) in the unskilled left batter.

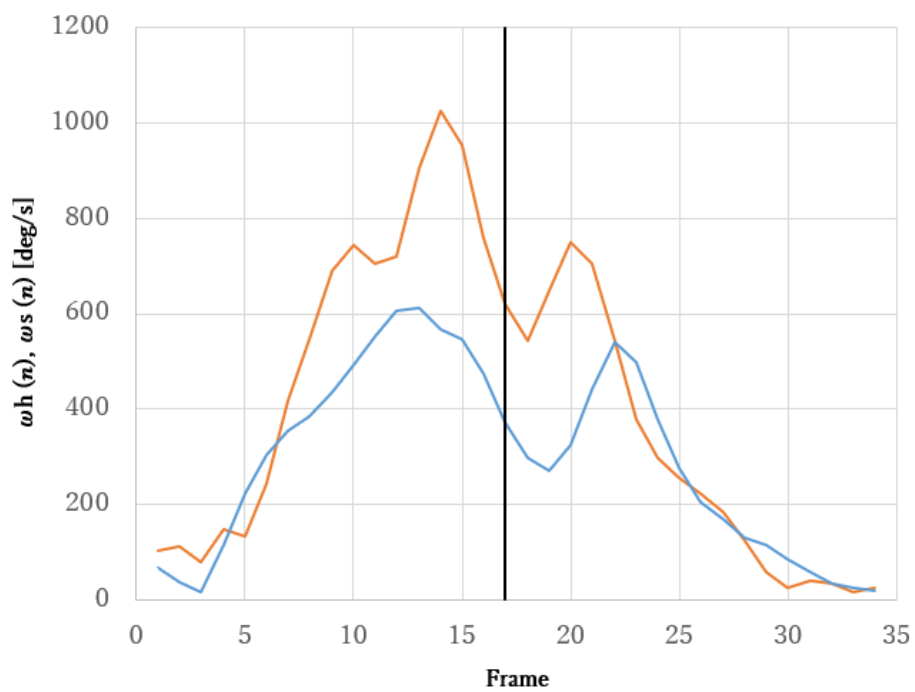


Figure 12: Rotation speed of hip (blue) and shoulder (orange) in the unskilled right batter.

before the wrist snap during the swing. Similarly, Figs. 15 and 16 show the tilt of the rotation planes for unskilled players.

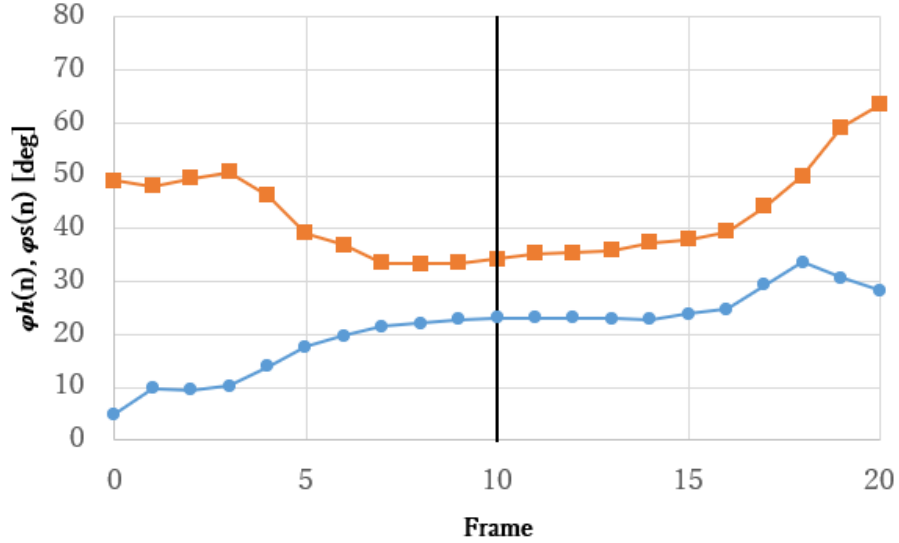


Figure 13: Inclination of rotation axis of hip (blue) and shoulder (orange) in the skilled left batter.

5 Discussions

The differences between skilled and unskilled players in terms of hip and shoulder rotation during the batting motion are outlined below.

- A) *Wrist snap timing and maximum shoulder rotation speed*
- B) *Stability of the hip and shoulder rotation axis*

5.1 Wrist snap timing and maximum shoulder rotation speed

For the skilled players, the shoulder rotation speed peaks at or just after the moment of the wrist snap. Figs. 9 and 10 show that the peaks of both skilled players' shoulder rotation are 1 frame after the wrist snap. In contrast, for unskilled players, the shoulder rotation speed begins to slow down at the moment of the wrist snap. Figs. 11 and 12 show that the peaks of both unskilled players' shoulder rotation are 3 frame before the wrist snap.

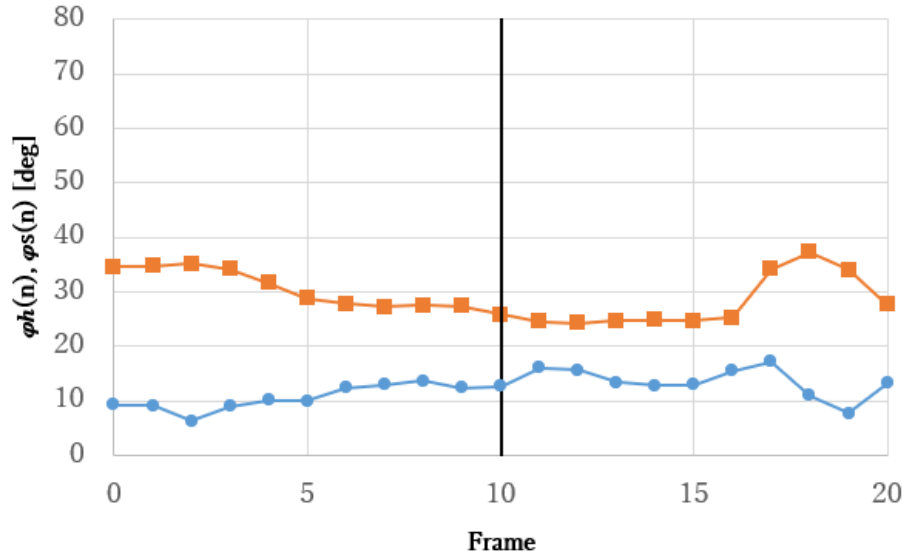


Figure 14: Inclination of rotation axis of hip (blue) and shoulder (orange) in the skilled right batter.

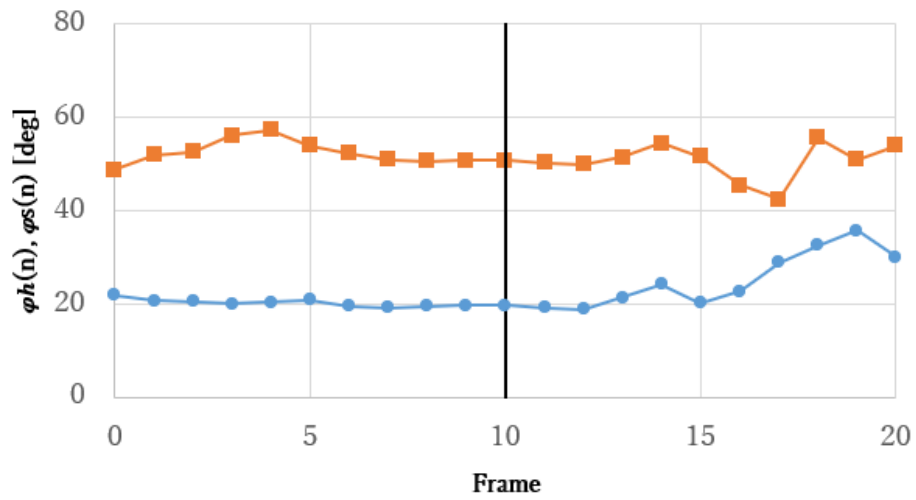


Figure 15: Inclination of rotation axis of hip (blue) and shoulder (orange) in the unskilled left batter.

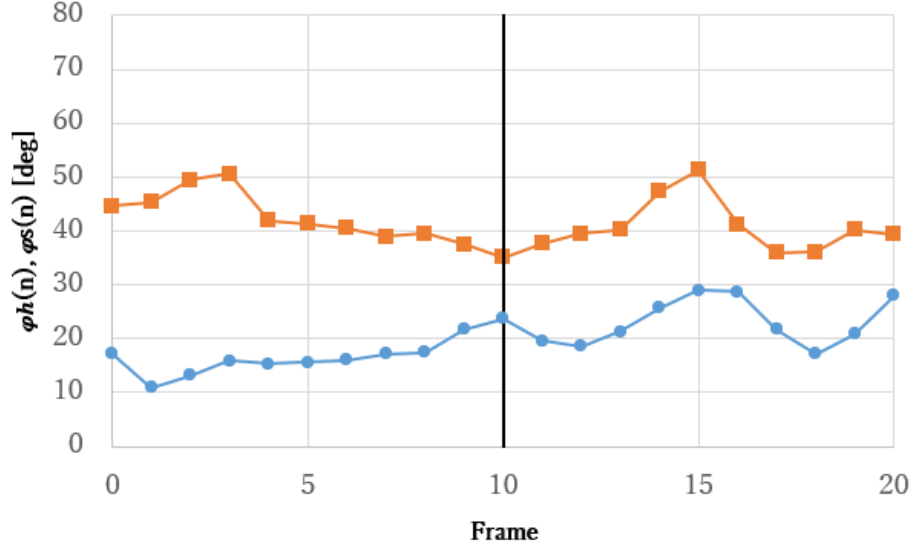


Figure 16: Inclination of rotation axis of hip (blue) and shoulder (orange) in the unskilled right batter.

5.2 Stability of the hip and shoulder rotation axis

Skilled players maintain a stable rotation axis during the 11 frames surrounding the impact. In contrast, unskilled players show a greater tilt in the shoulder rotation axis, and both the hip and shoulder rotation axes show significant variability. Table 1 summarizes the angles of the hip and shoulder rotation planes relative to the horizontal plane (mean \pm standard deviation) for the 5 frames before and 5 frames after, totally 11 frames around the wrist snap.

Table 1: Mean \pm standard deviation of rotation plane tilt.

	φ_h [deg]	φ_s [deg]
skilled, left	22.1 \pm 1.8	35.7 \pm 2.0
skilled, right	13.2 \pm 1.6	26.1 \pm 1.6
unskilled, left	20.1 \pm 1.5	51.6 \pm 1.5
unskilled, right	20.5 \pm 4.3	40.8 \pm 4.6

With the relative angle $\psi(n)$ between the rotation planes of hip and shoulder for frame n , the following equation is satisfied,

$$\cos(\psi(n)) = \vec{a}_s(n) \cdot \vec{a}_h(n).$$

Fig. 17 illustrates the relative angle $\psi(n)$. Fig. 18 shows the relative angles of the four players. Frame 5 represents the wrist snap of each player. Skilled

players are shown as straight lines and unskilled players are shown as dashed lines.



Figure 17: Relative angle ψ between hip and shoulder rotation axes.

6 Conclusion

The purpose of this study was to analyze time-series patterns of the rotational axes and angles of the waist and shoulders during a batter's swing. A motion capture system was used to collect swing data and to visualize the kinetic chain of the most important rotational movements, hip and shoulder rotation.

The analysis revealed significant differences between skilled and unskilled participants, particularly in (A) shoulder rotational velocity at the moment of wrist rotation and (B) stability of the waist and shoulder rotational axes. In addition, the experiment revealed individual differences in the use of the hip and shoulders. By visualizing the coordinated movement of the body during swing and comparing swing movements, this study provided insight into swing mechanics.

For further improvement, future challenges include increasing the number of participants to ensure statistically significant differences by comparing two groups, skilled and unskilled players. The population size of skilled players is approximately 30,000 including NPB, Nippon Professional Baseball, and college league baseball players. The general population of the same age group in Japan as unskilled players is approximately 10 million. Considering these population sizes, statistical significance is achieved with a sample size of 12 to 30 partici-

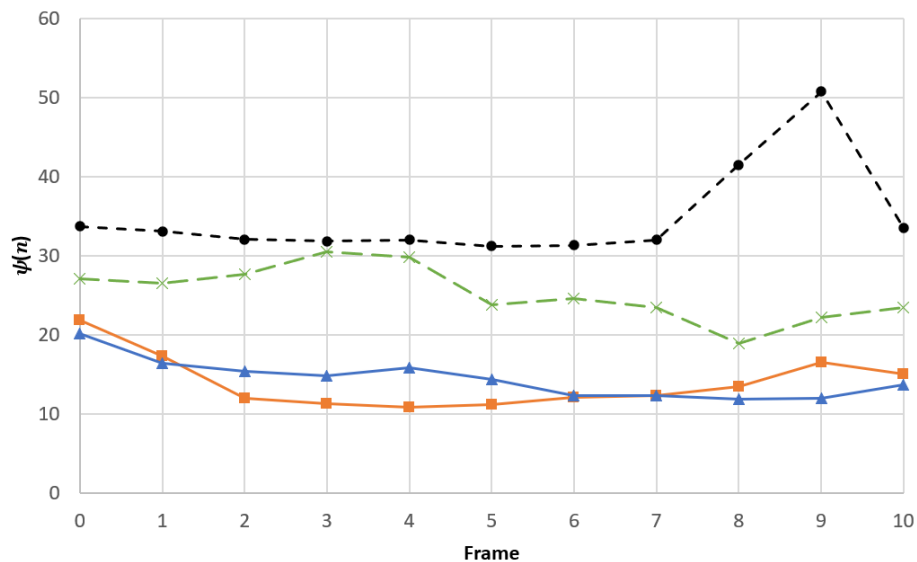


Figure 18: Relative angle ψ of rotation axes for skilled and unskilled players.

pants per group. Also, increasing the number of swing trials will contribute to investigate both inter- and intra-individual variation.

References

- [1] D. Hirayama, K. Yoshizawa, H. Sogo, and T. Henmi, “Quantitative comparison of technical differences in baseball batting motion by motion analysis,” in *2016 International Conference on Advanced Mechatronic Systems (ICAMechS)*, 2016, pp. 115–120.
- [2] M. Isogai, H. Kashiwazaki, K. Takahashi, and K. Miyawaki, “Ground reaction force evaluation during a baseball practice swing movement,” in *The 32nd 2021 International Symposium on Micro-NanoMechatronics and Human Science*, 2021, pp. 1–5.
- [3] H. N. Gen Horiuchi and S. Sakurai, “Mechanical energy flow in the lower extremities and torso during baseball batting,” *Japan J. Phys. Educ. Hlth. Sport Sci.*, vol. 62, no. 2, pp. 575–586, 2017.
- [4] C.-C. Fang, C.-H. Hsu, C.-W. Chiu, J.-T. Kung, and H.-C. Shih, “Center of mass trajectory: An image descriptor for baseball swing analysis based on single low-cost camera,” in *2021 IEEE International Conference on Multimedia & Expo Workshops (ICMEW)*, 2021, pp. 1–5.
- [5] T. Ishikawa and T. Murakami, “An approach to 3d gyro sensor based motion analysis in tennis forehand stroke,” in *IECON 2015 - 41st Annual*

Conference of the IEEE Industrial Electronics Society, 2015, pp. 002 354–002 359.

- [6] H. Zhao, S. Wang, G. Zhou, and W. Jung, “Tenniseye: Tennis ball speed estimation using a racket-mounted motion sensor,” in *2019 18th ACM/IEEE International Conference on Information Processing in Sensor Networks (IPSN)*, 2019, pp. 241–252.
- [7] A. Özçelik, “Rekreatif seviye kadın tenis oyuncularında forehand ve backhand vuruş performansları ile sweet-spot skorları arasındaki ilişkinin belirlenmesi,” *Ulusal Spor Bilimleri Dergisi*, vol. 7, no. 1, p. 12–21, 2023.
- [8] C. J. Ebner and R. D. Findling, “Tennis stroke classification: Comparing wrist and racket as imu sensor position,” in *Proceedings of the 17th International Conference on Advances in Mobile Computing & Multimedia*, ser. MoMM2019. New York, NY, USA: Association for Computing Machinery, 2020, p. 74–83. [Online]. Available: <https://doi.org/10.1145/3365921.3365929>
- [9] N. Reintrakulchai and W. Kimpan, “The design of golf swing pattern analysis from motion sensors,” in *2014 International Computer Science and Engineering Conference (ICSEC)*, 2014, pp. 222–227.
- [10] T. T. Kim, M. A. Zohdy, and M. P. Barker, “Applying pose estimation to predict amateur golf swing performance using edge processing,” *IEEE Access*, vol. 8, pp. 143 769–143 776, 2020.
- [11] Z. Zhang, Y. Zhang, A. Kos, and A. Umek, “Strain gage sensor based golfer identification using machine learning algorithms,” *Procedia Computer Science*, vol. 129, pp. 135–140, 2018, 2017 INTERNATIONAL CONFERENCE ON IDENTIFICATION, INFORMATION AND KNOWLEDGE IN THE INTERNET OF THINGS. [Online]. Available: <https://www.sciencedirect.com/science/article/pii/S1877050918302850>
- [12] Y. J. Kim, K. D. Kim, S. H. Kim, S. Lee, and H. S. Lee, “Golf swing analysis system with a dual band and motion analysis algorithm,” *IEEE Transactions on Consumer Electronics*, vol. 63, no. 3, pp. 309–317, 2017.
- [13] K. M. Curtis, M. Kelly, and M. P. Craven, “Cricket batting technique analyser/trainer using fuzzy logic,” in *2009 16th International Conference on Digital Signal Processing*, 2009, pp. 1–6.
- [14] I. Bandara and B. Bačić, “Strokes classification in cricket batting videos,” in *2020 5th International Conference on Innovative Technologies in Intelligent Systems and Industrial Applications (CITISIA)*, 2020, pp. 1–6.
- [15] S. Gajanayake, P. Karunaratne, and S. Fernando, “Development of an embedded device to characterize the orientation of a cricket bat in three-dimensional space,” in *2021 IEEE 16th International Conference on Industrial and Information Systems (ICIIS)*, 2021, pp. 336–340.

- [16] S. C. Mohonta and A. K. Sarkar, "Assessment of repetitive straight drive cricket batting using inertial sensor and pendulum dynamics," in *2015 International Conference on Electrical & Electronic Engineering (ICEEE)*, 2015, pp. 273–276.
- [17] N. Taguchi, K. Kaneoka, S. Izumi, and S. Miyakawa, "Analysis of trunk rotation during the baseball batting motion," *The journal of Japanese Society of Clinical Sports Medicine*, vol. 27, no. 1, pp. 11–19, 1 2019.